Spatial Distribution of Landslide Dams Triggered by the 2008 Wenchuan Earthquake

Xuanmei Fan, Cees J. van Westen, Qiang Xu, Tolga Gorum, Fuchu Dai, Gonghui Wang, and Runqiu Huang

Abstract

Landslide dams are a common type of river disturbance in tectonically active mountain belts with narrow and steep valleys. Here we present an unprecedented inventory of 828 landslide dams triggered by the 2008 Wenchuan earthquake, China. Of the 828 landslide dams, 501 completely dammed the rivers, while the others only caused partial damming. The spatial distribution of landslide dams was similar to that of the total landslide distribution, with landslide dams being most abundant in the steep watersheds of the hanging wall of the Yingxiu-Beichuan Thrust Fault, and in the northeastern part of the strike-slip fault near Qingchuan. We analyzed the relation between landslide dam distribution and a series of seismic, topographic, geological, and hydrological factors.

Keywords

Landslide • Landslide dam • Wenchuan earthquake • Spatial distribution

X. Fan (✉)
Faculty of Geo-Information Science and Earth Observation (ITC), University of Twente, P.O. Box 217, Enschede 7500 AE, The Netherlands

The State Key Laboratory of Geohazards Prevention and Geoenvironment Protection, Chengdu University of Technology, Chengdu, Sichuan, China
e-mail: fan21676@itc.nl

C.J. van Westen • T. Gorum • R. Huang
Faculty of Geo-Information Science and Earth Observation (ITC), University of Twente, P.O. Box 217, Enschede 7500 AE, The Netherlands

Q. Xu
The State Key Laboratory of Geohazards Prevention and Geoenvironment Protection, Chengdu University of Technology, Chengdu, Sichuan, China

F. Dai
Institute of Geology and Geophysics, Chinese Academy of Sciences, Beijing, China

G. Wang
Disaster Prevent Research Institute, Kyoto University, Uji, Kyoto, Japan

Introduction

Landslide dams are a common type of river disturbance in tectonically active mountain belts with narrow and steep valleys (Costa and Schuster 1988; Chai et al. 1995; Hewitt 1998). Besides a number of landslide-dam inventories (Costa and Schuster 1988, 1991; Chai et al. 1995; Casagli and Ermini 1999; Korup 2004), there are also many case studies (e.g. Dunning et al. 2005; Harp and Crone 2006; Nash et al. 2008; Duman 2009; Schneider 2009). Most studies use a geomorphic approach to analyze the characteristics of the landslides, dams, rivers and impounded lakes (e.g. Ermini and Casagli 2003; Korup 2004; Dong et al. 2009). Research on landslide dams has been reviewed by Korup (2002). However, there is hardly any work specifically on earthquake-induced landslide dams (Adams 1981; Hancox et al. 1997), due to the scarcity of well-documented inventories.

The devastating Wenchuan earthquake (Mw 7.9) with a focal depth of ~14 km to 19 km occurred on the NE-trending Longmenshan thrust fault zone, which separates the Sichuan basin from the eastern margin of the Tibetan Plateau. This fault zone consists of three major subparallel faults: the Wenchuan-Maowen, Yingxiu-Beichuan and Pengguan faults

Fig. 1 Distribution map of
landslides and landslide dams
triggered by the Wenchuan
earthquake. The Danguangbao
landslide is indicated with a
triangle. The white areas are
unmapped due to the presence of
clouds and shadows in the post-
earthquake images. The
following faults are indicated:
WMF Wenchuan-Maowen fault,
YBF Yingxiu-Beichuan fault, *PF*
Pengguan fault, *JGF* Jiangyou-
Guanxian fault, *QCF* Qingchuan
fault, *HYF* Huya fault, *MJF*
Minjiang fault (After Xu et al.
2009). The rivers indicated in the
figures are *MJR* Minjiang River,
MYR Mianyuan River, *JJR*
Jianjiang River, *QR* Qingzhu
River. The epicenter location is
from (USGS 2008)
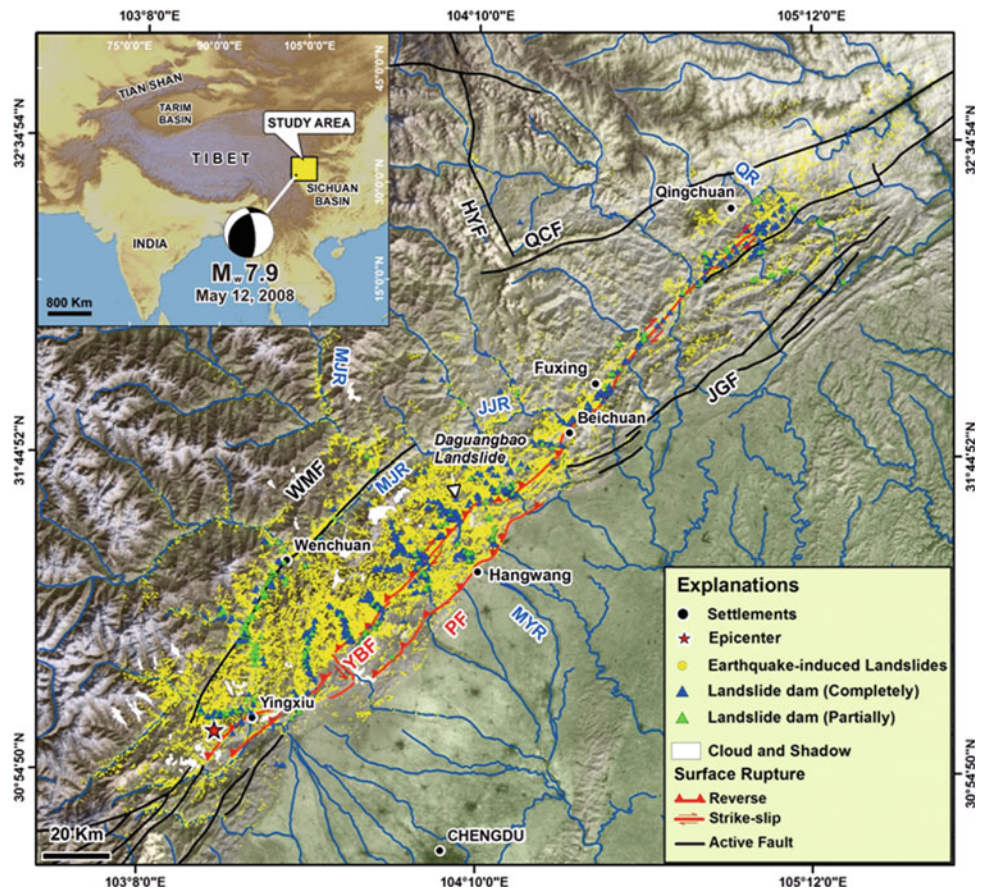
(Fig. 1). The coseismic rupture initiated near Yingxiu town
(31.0610N, 103.3330E) and propagated unilaterally towards
the northeast, generating a 240-km long surface rupture
along the Yingxiu Beichuan fault, and a 72-km long rupture
along the Pengguan fault (Xu et al. 2009; Lin et al. 2009;
Shen et al. 2009). GPS and InSAR data helped quantify the
variability of fault geometry and slip rate distribution (Yarai
et al. 2008; Hao et al. 2009), showing that in the southwest
(from Yingxiu to Beichuan) the fault plane dips moderately
to the northwest, becoming nearly vertical in the northeast
(from Beichuan to Qingchuan region), associated with a
change from predominantly thrusting to strike-slip motion.
The fault zone runs through a mountain range with elevations
ranging from 500 m in the Sichuan Basin to over 5,000 m
over a distance of ~50 km. Slope gradients within in the
deeply dissected fault zone are steep, commonly > 300.

    The Wenchuan earthquake provides a unique opportunity
to study the co-seismic landslide dams, since several
hundreds of landslide dams and over 60,000 landslides
were triggered (Gorum et al. 2011). This study aims to
present an unprecedented inventory and analyse the spatial
distribution of landslide dams triggered by the Wenchuan
earthquake, derived from detailed remote sensing interpreta-
tion and fieldwork. We focus on the relation between land-
slide dam distribution and a series of seismic, topographic,

geological, and hydrological factors, aiming to create a land-
slide dam susceptibility model by the multivariate statistical
method in future.

Event-Based Mapping of Landslide Dams

Event-based landslide mapping is usually carried out after
single landslide triggering events, such as an earthquake, an
intense rainfall event or a serious snowmelt event. It is a
mandatory step for analyzing the landslide distribution
(Harp and Jibson 1996; van Westen et al. 2008).

Source Data for Landslide Dam Mapping

In a previous study Gorum et al. (2011) presented the method
for mapping all landslides in the earthquake affected region
using 52 pre- and post earthquake satellite images. The same
data was used in this study for mapping the landslide dams,
including pre- and post- earthquake ASTER (15 m), ALOS
AVNIR-2 (10 m) and PRISM (2.5 m), Indian Cartosat-1
(2.5 m), SPOT-5 (2.5 m), IKONOS (2.5 m), as well as a
number of aerial photos (0.3 m). In addition, a pre-
earthquake DEM was used, which was generated from

1:50,000 scale digital topographical maps. Unfortunately insufficient data was available for generating a post-earthquake DEM, so that volume analysis was not possible.

Mapping and Interpretation Method

Landslide dams were mapped through visual interpretation by comparing pre- and post-earthquake images, assisted by field checks in accessible areas. The "fresh" landslides are clearly recognizable change detection of the monoscopic images also allowed to achieve good results by making optimal use of image characteristics such as tone, texture, pattern and shape.

Landslides were identified which blocked the rivers completely or partially, and for these the initiation and runout areas were mapped as polygons, as well as the associated barrier lakes. The polygon mapping was done first using medium resolution images (ASTER and ALOS AVNIR-2), and was refined for those areas where also high resolution images were available (ALOS PRISM, Cartosat-1, SPOT-5, IKONOS an Airphotos). Figure 1 shows the distribution of the landslide dams, plotted on a map with the overall landslide distribution made by Gorum et al. (2011). Figure 2 gives an example of the use of medium and high resolution imagery for landslide dam mapping. On the medium resolution images, the landslide initiation and runout areas cannot be mapped as separate polygons (Fig. 2 a, c), whereas this is possible using high resolution images (Fig. 2 b, d).

Landslide dams can be easily identified by a number of diagnostic features. They have a higher reflectance rate compared to the surrounding areas with vegetation cover, and often show clear geomorphological characteristics, such as scarps, rock fall talus, flow lobes, hummocky and asymmetric deposits, transverse depression and an elongated shape downslope. A very important characteristic is the disruption of surface drainage, by partially or completely blocking the river below. The presence of a barrier lake is certainly the most important characteristic, although this was not the case for many of the identified landslide dams as the damming had been partially, or the dam had already broken.

In total, 828 landslide dams were mapped. Of them, 501 completely dammed the rivers with a total area of 23.7 km^2, while the others only caused partial damming.

Analysis of Landslide Dam Spatial Distribution

Gorum et al. (2011) concluded that the distribution pattern of landslides triggered by the Wenchuan earthquake is primarily controlled by the coseismic slip rate distribution, the fault geometry and characteristics. We found that landslide distribution in the section of the fault that had mainly
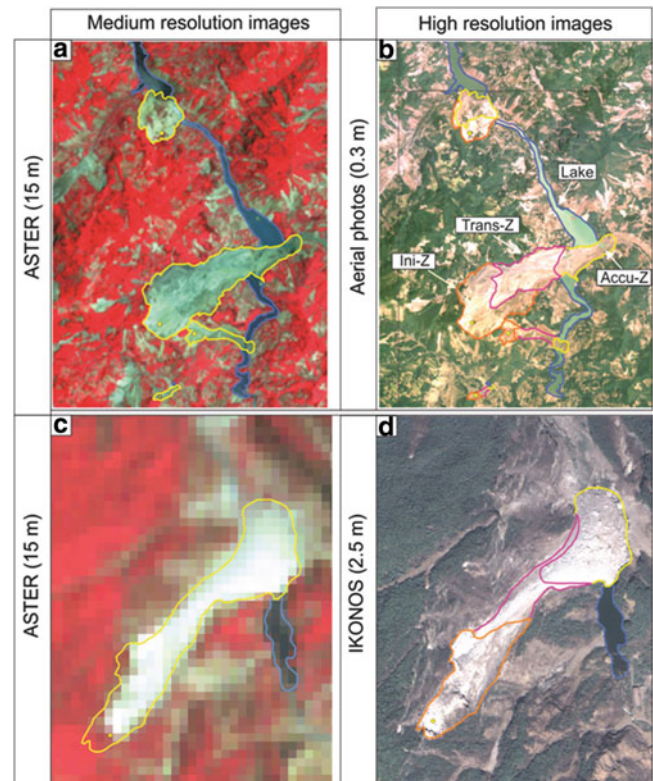

Fig. 2 Examples of medium (*left*) and high (*right*) resolution images showing landslide dam polygon mapping. Detailed mapping allowed delineating the initiation (Ini-Z), transportation (Trans-Z) and accumulation (Accu-Z) parts of damming landslides, whereas the landslides can only be mapped as single polygons using medium resolution images

a thrust component with a low angle fault plane was much higher than the sections that had steeper fault angles and a major strike slip component. Figure 1 shows that areas with a high landslide density in the vicinity of rivers are prone to produce a high density of landslide dams. There are relatively many landslide dams along the deeply-incised Minjiang River, of which most are partially damming due to the high discharge and erosive capacity. The landslide dams are distributed in a relative wider region with comparatively higher density in the SW from the epicenter to Beichuan town and around the end of the main fault in Qingchuan. Around 70 % of landslide dams concentrated in the Pengguan Massif along the fault thrust component, mainly due to two reasons: (1) this region has a high landslide density; (2) the traverse rivers in the Pengguan Massif has smaller catchment area than the Minjiang river and Jianjiang river, thus, the smaller discharge and river width (Kirby and Whipple 2003).

The spatial distribution of landslide dams is controlled by several seismic and geo-environmental factors (Keefer 2000). We will analyze the variation of landslide dam distribution with aforementioned factors to statistically evaluate the impacts of these factors on landslide dam distribution.
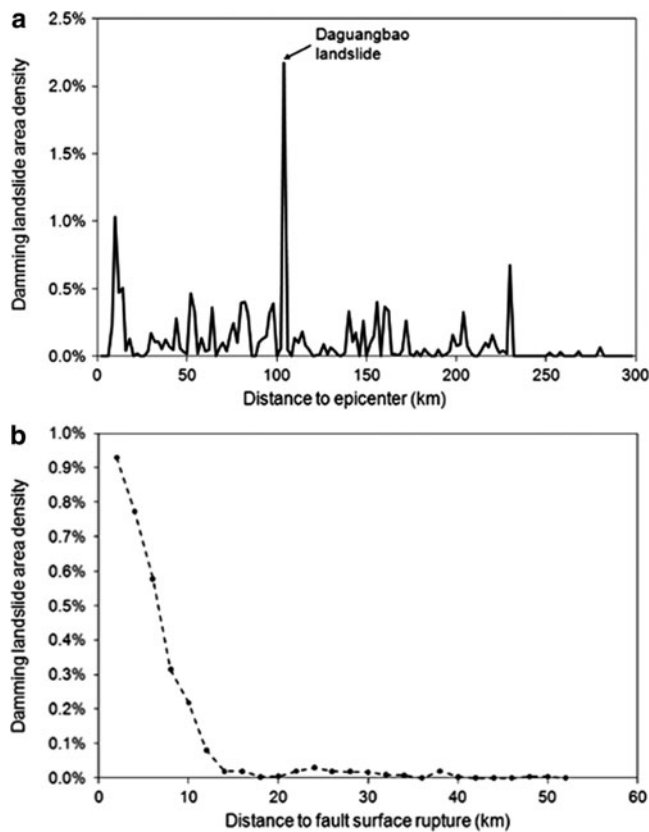
Fig. 3 (**a**) Damming landslide area density versus Distance to epicentre; (**b**) Damming landslide area density versus Distance to fault surface rupture

Fig. 4 (**a**) Frequency distribution of slope gradient and damming landslide ratio; (**b**) Frequency distribution of internal relief and damming landslide ratio

Variation of Damming Landslide Occurrence with Seismic Factors

We selected two most commonly used factors, the distance to epicenter and to the fault surface rupture to analyze the relation of landslide dam occurrence with seismic factors. The damming landslide area density (LDAD) was determined for a sequence of concentric bands 2 km wide extending outward from the seismic source in ArcGIS. Figure 3a shows the variation of LDAD with epicentre distance. A obvious peak with the LDAD value of 2.17 % was caused by the largest landslide, the Daguangbao landslide in the study area. The Daguangbao landslide has an area of 7.1 km^2 and an estimated volume of 7.5 × 10^8 m^3 (Huang et al. 2011) to 8.4 × 10^8 m^3 (Chigira et al 2010). The damming landslide area density (LDAD) didn't show a clear decay relationship with the distance to epicenter. It means that the distance to epicenter is not a control factor for landslide dam generation. Differently, with the increase of distance to the fault surface rupture, the LDAD decreased significantly, from 0.93 % at 2 km distance to 0.004 % at 50 km, but the decay rate become slight after 12 km (Fig. 3b).
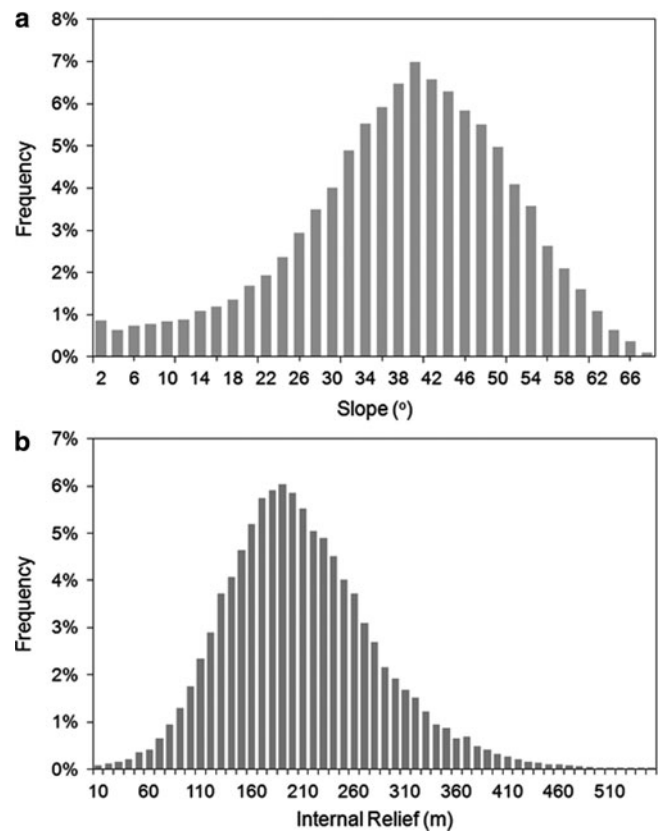
Variation of Damming Landslide Occurrence with Terrain Factors

We considered the slope gradient, internal relief, altitude, slope aspect, profile curvature and plan curvature as the main terrain factors, which can be extracted from 25-m DEM. The slope gradient and internal relief seems to be more important than others (Fig. 4). In the study area, the mean altitude value is calculated as 2,361 m, on the grid cells with landslides the average value is obtained as ~1,900 m (Gorum et al. 2011). The damming landslides are most abundant between altitude 700 m and 1,700 m, which are lower than the mean altitude of landslides, because damming landslides more densely distributed in the hill slopes in the vicinity of rivers. There is no preferential aspect for damming landslides, since it might more depend on the river direction. The rest of factors, such as the plan and profile curvature do not show clear relationship with landslide dam occurrence. The frequency distribution of slope gradient and internal relief was plotted in Fig. 4 a, b, which indicates that most abundant damming landslides with the slope gradient of ~40° and the internal relief of ~180 m.
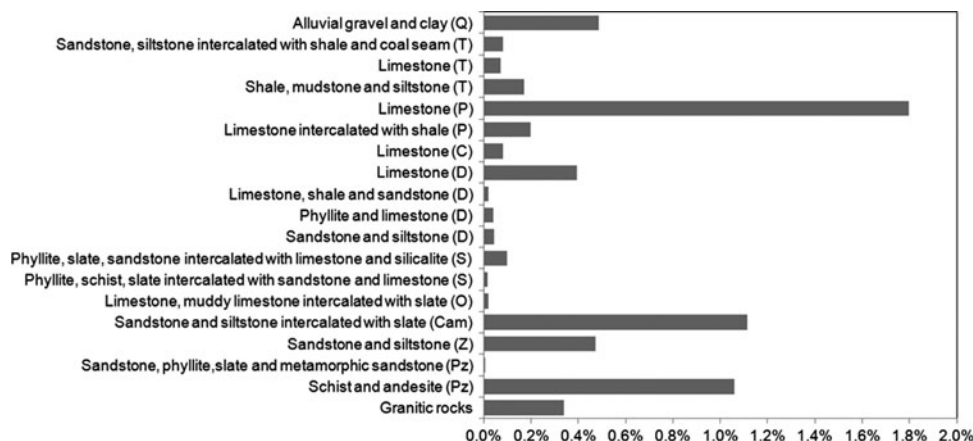
Fig. 5 Damming landslide point and area densities for lithologic units

Variation of Damming Landslide Occurrence with Lithology

Lithology is considered the most important geological factor. In this study, a geological map was compiled from ten 1: 200,000 scale standard geological maps. The landslide dam area density (LDAD) was determined for each lithologic unit (Fig. 5). The lithology of damming landslides varies from Quaternary alluvial gravel and clay to Pre-Sinian rocks. A peak of LDAD value of 1.8 % appears in the Permian limestone, due to the contribution of the aforementioned Daguangbao landslide. The results show that the Cambrian sandstone and siltstone intercalated with shale, as well as the Pre-sinian schist and andesite have the relatively high damming landslide area density. The same rock types also produced high density of coseismic landslides, according to Dai et al. (2010). Field investigation also revealed that the Pre-sinian schist is very weak and fractured, producing a large amount of landslides. The shale intercalated in sandstone and siltstone of the Cambrian age largely affects the integrity and strength of the slopes, resulting in the high density of landslides and landslide dams. Limestone and limestone intercalated with shale are generally well stratified and densely jointed, generating both deep-seated rockslides on cataclinal slopes and shallow rockslides or rock falls on anaclinal slopes. Chigira et al (2010) found that many of the sliding surfaces in carbonate rocks had rough surfaces with dimple-like depressions by dissolution. Large rock avalanches were mostly observed in the intensely cracked granitic rock masses as well as sandstones and siltstones.

Variation of Damming Landslide Occurrence with Hydrological Factors

Hydrological factors play important roles in landslide dam formation, such as the distance to streams, stream order,

upper catchment area, stream power index etc. Here, we focus on the distance to streams and stream order. Figure 6 shows that generally with the increase of landslide distance to streams, the damming landslide number decreases. Over 80 % of damming landslides concentrated within 400 m distance to the streams. Besides, the average area of damming landslides shows an increasing trend with the increase of the distance to streams. It implies that the farther away from the river, the larger the landslide is required to block a river and form a dam.

The stream order was calculated by the method proposed by Strahler (1957) using SAGA software (System for Automated Geoscientific Analyses). Figure 7 depicts that ~90 % of damming landslides occur along the rivers with stream order varying from 1 to 3. The stream order reflects the stream power of a river. The higher the stream order, the more powerful the river is. Therefore, the damming landslide frequency decreased significantly, when the stream order increased from 2 to 6. However, few damming landslides occurred along the river with stream order of 1, because those low stream order rivers are the small tributaries at the initial (upper) part of catchments, thus, with very low discharge and incision. The area range of damming landslides with each stream order was represented by box plot in Fig. 7, which indicates a general trend that the higher the stream order, the larger the landslide is required to block a river. However, this trend is not so pronounced when the stream order varies from 1 to 3, as it does from 4 to 6.

Conclusions

Temporary or permanent blockage of stream by landslides is a serious secondary hazard in mountainous areas that are affected by strong earthquakes or major rainfall events. They may pose a large risk to downstream areas as a result of catastrophic lake outbreak flooding. This phenomenon has gradually received more attention in literature, although several issues are still poorly
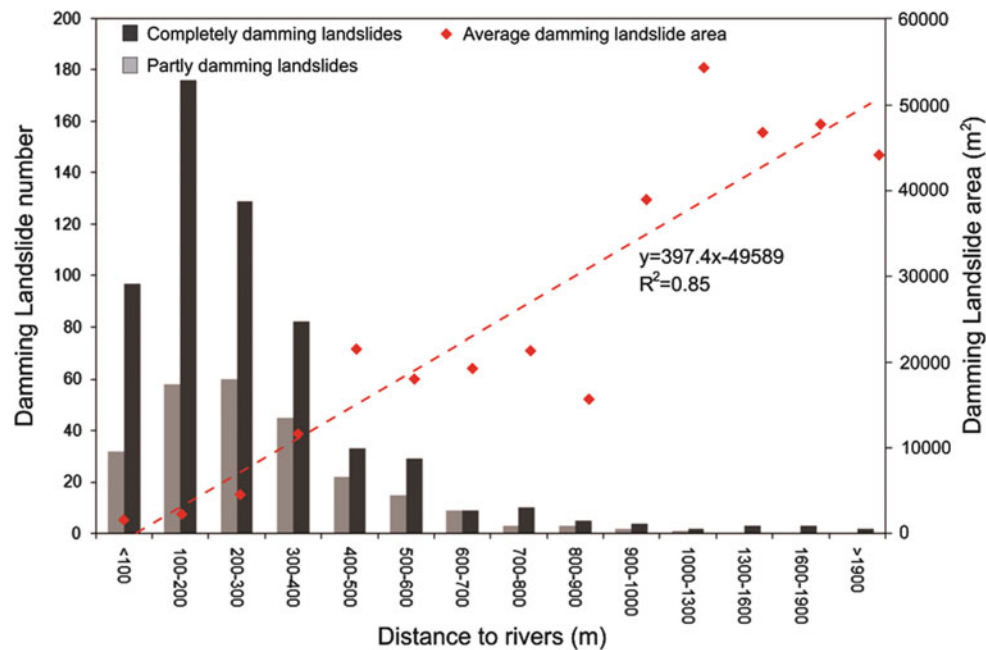
Fig. 6 Relationship between damming landslide number, average area and distance to rivers
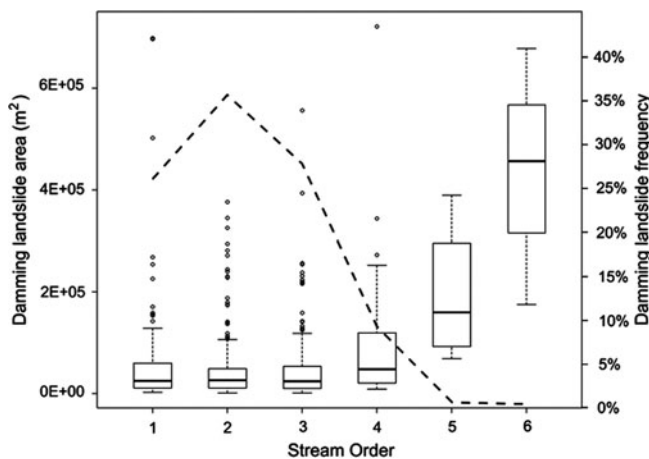

Fig. 7 Relationship between damming landslide frequency (represented by the *dash line*), area and stream order. The boxes and whiskers show ranges of damming landslide area for each stream order. *Black circles* are the outliers. *Horizontal line* defines the median

for a single triggering event, and use it to analyze the spatial distribution of landslide dams and the related controlling factors, including the seismic, terrain, lithologic and hydrological parameters. Next site-specific details such as the valley geomorphometry and stream discharge should also be taken into account. The ultimate aim is to combine this with earthquake acceleration modelling and landslide hazard assessment in order to provide a probabilistic landslide dam hazard assessment.

understood, such as the landslide dam formation conditions, dam classification, and in particular landslide dam susceptibility and hazard assessment. To understand these aspects better research on individual datasets of landslide dams caused by the same triggering event is important.

The Wenchuan earthquake provided the opportunity to generate an event-based landslide dam inventory of 828 individual landslide dams, of which 501 caused the complete blockage of the drainage. In this study, efforts were paid to create an almost complete landslide dam database

References

Adams J (1981) Earthquake-dammed lakes in New Zealand. Geol Soc Am Geol 9:215–219

Casagli N, Ermini L (1999) Geomorphic analysis of landslide dams in the Northern Apennine. Trans Jpn Geomorphol Union 20:219–249

Chai HJ, Liu HC, Zhang ZY (1995) The catalog of Chinese landslide dam events. J Geol Hazard Environ Preserv 6(4):1–9, In Chinese

Chigira M, Xu XY, Inokuchi T, Wang GH (2010) Landslides induced by the 2008 Wenchuan earthquake, Sichuan, China. Geomorphology 118(3–4):225–238

Costa JE, Schuster RL (1988) The formation and failure of natural dams. Geol Soc Am Bull 100:1054–1068

Costa JE, Schuster RL (1991) Documented historical landslide dams from around the world, vol 91–239, U.S. geological survey open-file report. U.S. Geological Survey, Vancouver, 486p

Dai FC, Xu C, Yao X, Xu L, Tu XB, Gong QM (2010) Spatial distribution of landslides triggered by the 2008 Ms 8.0 Wenchuan earthquake, China. J Asian Earth Sci. doi:10.1016/j.jseaes.2010.04.010

Dong JJ, Tung YH, Chen CC, Liao JJ, Pan YW (2009) Discriminant analysis of the geomorphic characteristics and stability of landslide dams. Geomorphology 110:162–171

Duman TY (2009) The largest landslide dam in Turkey: Tortum landslide. Eng Geol 104:66–79

Dunning SA, Petley DN, Rosser NJ (2005) The morphology and sendimentology of valley confined rock-avalanche deposits and their effect on potential dam hazard. In: Hungr O, Fell R, Couture R, Eberhardt E (eds) Landslide risk management. Taylor & Francis, London. ISBN 04 1538 043X

Ermini L, Casagli N (2003) Prediction of the behavior of landslide dams using a geomorphological dimensionless index. Earth Surf Process Landf 28:31–47

Gorum T, Fan XM, van Westen CJ, Huang RQ, Xu Q, Tang C, Wang GH (2011) Distribution Pattern of Earthquake-induced Landslides Triggered by the 12 May 2008 Wenchuan Earthquake. Geomorphology. doi:10.1016/j.geomorph.2010.12.028

Hancox GT, Perrin ND, Dellow GD (1997) Earthquake-induced landsliding in New Zealand and implications for MM intensity and seismic hazard assessment. Institute of Geological and Nuclear Sciences Client Report 43601B prepared for Earthquake Commission Research Foundation, Lower Hutt, p 85

Hao KX, Si H, Fujiwara H, Ozawa T (2009) Coseismic surface-ruptures and crustal deformations of the 2008 Wenchuan earthquake Mw 7.9, China. Geophys Res Lett 36(11):2–6

Harp EL, Crone AJ (2006) Landslides triggered by the October 8, 2005, Pakistan earthquake and associated landslide-dammed reservoirs, vol 2006–1052, U.S. geological survey open-file report. U.S. Geological Survey, Reston, 13p

Harp EL, Jibson RW (1996) Landslides triggered by the 1994 Northridge, California earthquake. Bull Seismol Soc Am 86:319–332

Hewitt K (1998) Catastrophic landslides and their effects on the upper Indus streams, Karakoram Himalaya, northern Pakistan. Geomorphology 26:47–80

Huang RQ, Pei XJ, Fan XM, Zhang WF, Li SG, Li BL (2011) The characteristics and failure mechanism of the largest landslide triggered by the Wenchuan earthquake, May 12, 2008, China. Landslides. doi:10.1007/s10346-011-0276-6

Keefer DK (2000) Statistical analysis of an earthquake-induced landslide distribution-the 1989 Loma Prieta, California event. Eng Geol 58:231–249

Kirby E, Whipple KX (2003) Distribution of active rock uplift along the eastern margin of Tibetan Plateau: Inferences from bedrock channel longitudinal profiles. J Geophys Res 108:1–24

Korup O (2002) Recent research on landslide dams-a literature review with special attention to New Zealand. Prog Phys Geogr 26:206–235

Korup O (2004) Geomorphometric characteristics of New Zealand landslide dams. Eng Geol 73:13–35

Lin A, Ren Z, Jia D, Wu X (2009) Co-seismic thrusting rupture and slip distribution produced by the 2008 Mw 7.9 Wenchuan earthquake, China. Tectonophysics. doi:10.1016/j.tecto.2009.02.014

Nash T, Bell D, Davies T, Nathan S (2008) Analysis of the formation and failure of Ram Creek landslide dam, South Island, New Zealand. N Z J Geol Geophys 51:187–193

Schneider JF (2009) Seismically reactivated Hattian slide in Kashmir, Northern Pakistan. J Seismol 13(3):387–398

Shen Z, Sun J, Zhang P, Wan Y, Wang M, Bürgmann R, Zeng Y, Gan W, Liao H, Wang Q (2009) Slip maxima at fault junctions and rupturing of barriers during the 2008 Wenchuan earthquake. Nat Geosci 2:718–724. doi:10.1028/NGEO636

Strahler AN (1957) Quantitative analysis of watershed geomorphology. Trans Am Geophys Un 38:913–920

U.S. Geological Survey (2008) Magnitude 7.9 – Eastern Sichuan, China, 2008 May 12 06:28:01UTC. http://earthquake.usgs.gov/earthquakes/eqinthenews/2008/us2008ryan/

van Westen CJ, Castellanos E, Kuriakose SL (2008) Spatial data for landslide susceptibility, hazard, and vulnerability assessment: an overview. Eng Geol 102:112–131

Xu X, Wen X, Yu G, Chen G, Klinger Y, Hubbard J, Shaw J (2009) Coseismic reverse- and oblique-slip surface faulting generated by the 2008 Mw 7.9 Wenchuan earthquake, China. Geology 37:515–518

Yarai H, Nishimura T, Tobita M, Amagai T, Suzuki A, Suito H, Ozawa S, Imakiire T, Masaharu H (2008) A fault model of the 2008 Wenchuan earthquake estimated from SAR measurements. In: 7th Academic surgical congress meeting, X2-040, Reykjavik